ChemCatChem
Communications
doi.org/10.1002/cctc.202101224
Chemistry Europe
European Chemical Societies Publishing
www.chemcatchem.org

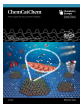

Hybrid Organic-Inorganic Heterogeneous Interfaces for Electrocatalysis: A Theoretical Study of CO_2 Reduction to C_2

Mingyu Wan,[a] Zhiyong Gu,[a] and Fanglin Che*[a]

Hybrid organic-inorganic heterogeneous catalytic interfaces, where traditional catalytic materials are modified with self-assembled monolayers (SAMs), create promising features to control a wide range of catalytic processes through the design of dual organic-inorganic active sites and the induced confinement effect. To provide a fundamental insight, we investigated CO_2 electroreduction into valuable C_2 chemicals (CO_2RR-to-C_2) over SAM-modulated Cu. Our theoretical results show that 1/4 monolayer aminothiolates improve the stability, activity and selectivity of CO_2RR-to-C_2 by: (1) decreasing surface energy to suppress surface reconstruction; (2) facilitating CO_2 activation and C–C coupling through dual organic-inorganic (i.e., –NH, Cu) active sites; (3) promoting C–C coupling via confinement effects that enlarge the adsorption energy difference between CO* and COH*; (4) inducing local electric fields to Cu surface and changing its dipole moment and polarizability to be in favor of C–C coupling under electrode/electrolyte interfacial electric field.

A critical component of the clean energy involves the capture and conversion of carbon dioxide (CO_2) produced from the combustion of fossil resources. One path to achieve low carbon emission chemical manufacturing is the electrochemically driven CO_2 reduction reaction (CO_2RR), which produces small building-block molecules (i.e., C_2 products, such as ethylene and ethanol) that are used widely in the manufacture of a broad range of chemicals and fuel products.[1] The desired goals for this technology, e.g., CO_2RR, are long-term stability, high electricity-to-chemical power energy efficiency and sustainable energy resilience.[2]

Traditional heterogeneous catalysts for CO_2RR-to-C_2 rely on purely inorganic components, i.e., metals, metal derivatives, alloys, and single-atom catalysts.[3] Although these catalysts exhibit moderate CO_2RR activities,[4] there are poor stabilities due to the surface reconstruction under high overpotential.[5] In particular, Cu is considered as one of the most promising and low-cost metal catalysts for CO_2RR to generate a valuable product spectrum.[6] However, Cu has two significant limitations with respect to CO_2RR-to-C_2: (1) CO_2 is a stable molecule containing two π bonds and has weak electronic interaction with Cu, meaning that a large overpotential needs to apply to activate CO_2, and thus, leading to a low CO_2RR current density;[7] (2) CO_2 reduction on Cu can produce a number of C_1 and C_2 products but the partial current density to only the valuable C_2 products is low.[3]

To mitigate the above challenges of Cu catalytic CO_2RR-to-C_2, one needs to (1) strengthen the electronic interaction between CO_2 (i.e., in the format of COOH[8]) and the catalytic adsorption site; and (2) tune the binding energy of CO*, which is the key intermediate to the C_2 products. Via confinement effects (i.e., confined space and confined electric fields) and the flexibility of the functional group of self-assembled monolayer (SAM), SAM has been widely used in thermal heterogeneous catalysis to tune the binding energy of the reactive species and subsequently, to control reaction activity and selectivity. For example, Medlin and co-workers[9] found that the confined space induced by C_{18} SAMs could enforce aromatic alcohol reactants to vertically adsorb over Pd catalytic surfaces, rather than their more thermodynamically favorable flat-on configurations. The activation energy for the hydrodeoxygenation (HDO) reaction was lowered and its competing decarbonylation reaction was suppressed by such upright orientations of aromatic alcohol reactants in the presence of C_{18} SAMs over Pd. With the flexible functional group of SAM, Ellis et al.[10] reported that SAM could regulate the electronic properties of surface sites, change TiO_2 surface's dipole moment, and thereby, improve the activity and selectivity of the desired dehydration reaction for 1-propanol and 1-butanol. Taken together, we designed the catalyst – aminothiolate SAM-modulated Cu (i.e., –S–C_2H_4–NH_2) – to enhance the CO_2RR-to-C_2 (Figure 1a). The reason of selecting amine as the functional group of SAM is that amine group could facilitate CO_2 capture and conversion,[11] which could potentially improve the current density of CO_2RR. In this study, we demonstrated that aminothiolate SAM-modulated Cu catalyst could facilitate CO_2-to-C_2 (Figure 1b) by: (1) suppressing surface reconstruction through decreasing surface energy, (2) promoting CO_2 activation via amine group, (3) inducing confinement effect to enlarge the adsorption energy difference between CO* and COH*, thus favoring carbon-carbon (C–C) coupling, which is the rate limiting step for C_2 species,[6,12] and (4) inducing confined electric field, changing surface dipole moment and polarizability to tune C–C coupling energetics under electric field.

To study the properties of the hybrid organic-inorganic interface for heterogeneous catalysis, we first determined the most favorable configurations for aminothiolate SAM-modulated Cu facets (Figure S1). Since different SAM surface cover-

[a] M. Wan, Dr. Z. Gu, Dr. F. Che
Chemical Engineering Department
University of Massachusetts Lowell
Lowell, MA-01854 (USA)
E-mail: fanglin_che@uml.edu

Supporting information for this article is available on the WWW under https://doi.org/10.1002/cctc.202101224

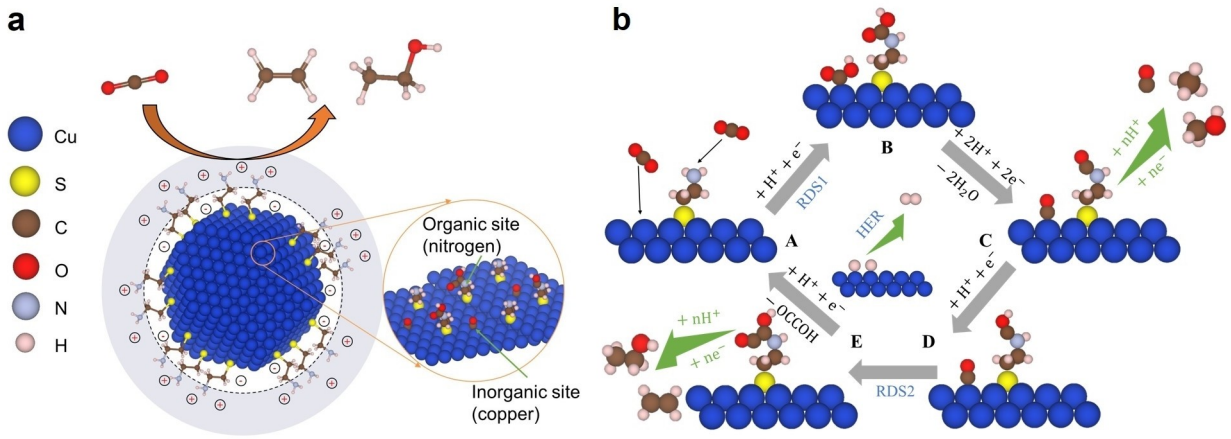

Figure 1. a Aminothiolate SAM-modulated Cu catalysts can provide dual organic-inorganic surface-active sites, induce local electric fields and change the surface dipole moment and polarizability, to accelerate CO_2RR-to-C_2. **b** A proposed schematic mechanism of CO_2RR to C_1 and C_2 with two possible rate-determining steps (RDS1 and RDS2) over the aminothiolate SAM-modulated Cu catalysts. The competitive reaction is hydrogen evolution reaction (HER). These three steps in blue are essential to be evaluated for this study.

ages over Cu might exist under electroreduction conditions and alter the reactivity,[13] we varied the surface coverages of SAM for Cu(100), Cu(111) and Cu(211) in our model (details of coverage selection refers to **Surface Coverages and Stabilities of Aminothiolates over Cu Catalysts** in SI). Aminothiolates preferentially adsorb at the four-fold hollow on Cu(100), three-fold hollow on Cu(111) and step-bridge site over Cu(211), respectively, at various examined coverages (i.e., 1/16 ML, 1/8 ML, 1/4 ML) (Figures S2–S4 and Table S1), which is consistent with the previous study.[14] All three Cu facets have very similar strong binding energies for aminothiolates (i.e., lower than −2 eV, Figure S5). As increasing the surface coverage of aminothiolates to 1/2 ML, Cu(100) shows the strongest adsorption energies of ~−1.7 eV (~−1.3 eV over Cu(211) and ~−0.6 eV over Cu(111)). Critically, when the SAM coverage is over 1/4 ML and the surface space is confined, the only remaining available Cu sites for reaction intermediates to adsorb and react over all three facets are the three and four-fold hollow sites. Thus, aminothiolate SAMs can induce confinement effects and selectively control the active surface sites by blocking nearby top and bridge sites while exposing only hollow sites.

The stability of the aminothiolate SAM-modulated Cu catalysts during reaction is influenced by both the adsorption of SAM and the surface formation energies of Cu. Thus, we evaluated surface formation energy in the presence and absence of aminothiolates at various surface coverages using Equation (S3) in the SI. DFT results show that the surface formation energies decrease as the surface coverage of aminothiolates over Cu increases, suggesting that a higher coverage of SAM is more stable than the lower surface coverage ones (Figure 2), which agrees well with the previous study regarding the stability of various surface coverages of short alkyl chain SAM over Cu(100).[15]

Due to the possibility for the reduction of surface aminothiolates to aminothiols and their subsequent desorption into

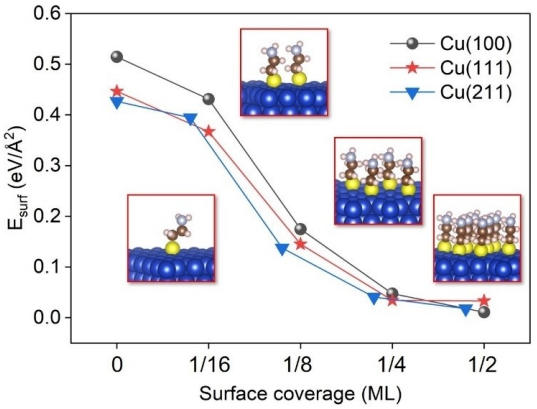

Figure 2. The surface formation energies of the most favorable geometries of aminothiolates over Cu with various surface coverages. The side view of aminothiolates over Cu(111) are inserted.

the reaction mixture under electroreduction conditions, we evaluated the stabilities of various surface coverages of aminothiolates over Cu under different electrochemical environments by calculating the free energy of aminothiolate reduction (the calculation details can refer to Equation (S4–S9) in SI). The results show that, under applied potential U_{SHE} of −1 V (estimated electrode potential of CO_2RR-to-C_2), only 1/16 ML aminothiolate over Cu is still stable at all pH; 1/8 ML and 1/4 ML of SAM are stable when pH is larger than 2; while 1/2 ML surface coverage of aminothiolate becomes unstable over Cu at all pH (Figure S6). Taken them together, under the CO_2RR-to-C_2 experimental conditions, 1/4 ML surface coverage of aminothiolates over Cu is more favorable to be present during the reaction.

Due to the different charges of the head and tail groups of organic aminothiolate SAM[10,15], it might induce high local electric fields, and change the surface dipole moment and polarizability, which could alter the electronic interactions

between adsorbates and the catalytic surface, influencing (electro)catalytic activity and selectivity.[16] To measure the possible local electric fields generated by aminothiolate SAMs on Cu, we modeled three kinds of aminothiolate SAMs (i.e., –NH, $–NH_2$ and $–NH_3$) at various surface coverages on Cu(100) (Figure 3a and 3c) because these three functional groups have different favorabilities under various electrochemical conditions (i.e., potential and pH). Based on our established Pourbaix diagram (Figure S7, detailed calculations are given by Equation (S10–S11) in the SI), under the basic solution (pH > 7) and the positive potentials ($U_{SHE} > 1.0$ V), the –NH thiolates could be thermodynamically stable; While under the acidic solution (pH < 7) and the applied negative potentials ($U_{SHE} < -1.5$ V), $–NH_3$ thiolates could be thermodynamically favorable. For our interested reaction of CO_2RR-to-C_2, it is usually operated under applied negative potentials of 0 to −1.5 V and neutral or basic pH solution,[12] $–NH_2$ thiolates over Cu are thermodynamically stable. Aminothiolate with the tail group of $–NH_3$ induces a 9-fold higher negative electric field as compared to that of $–NH_2$, whereas –NH induces a positive electric field (Figure 3a and 3b). As the surface coverage of aminothiolate SAMs with $–NH_3$ increases from 1/16 ML to 1/4 ML, the average negative electric field strength increases monotonically from 0.63 V/Å to 1.04 V/Å (Figure 3b). The near-surface local electric field strength induced by aminothiolates decreases dramatically as increasing the distance between the thiolates and adsorbed intermediates (Figure 3d). The introduction of SAMs with tunable tail groups and surface coverages over Cu also shifts the surface dipole moment and polarizability (Figure S8). $–NH_3$ aminothiolate SAM has the largest dipole moment of 1.76 eÅ and polarizability of 10.48 eÅ^2/V, compared to the other two aminothiolate SAMs. In addition, the dipole moment and polarizability decrease with increasing surface coverage of $–NH_3$ aminothiolate SAMs (Figure 3b and 3c). In summary, the tail functional group of SAMs and the surface coverage of SAMs change the local electric fields, surface instinct dipole and polarizability of the Cu catalysts. Similar observations were found in the literature from both experiment and theoretical perspectives. Dawlaty group[17] found that during surfactants modulated interfacial processes, cationic surfactants produced a larger effective interfacial field of ~−1.25 V/nm compared to anionic surfactants of ~0.4 V/nm. They also reported that such interfacial fields from cationic surfactants promoted CO_2RR to hydrocarbon products and suppressed hydrogen evolution reaction (HER). Chen et al. from theory perspective[18] and Gunathunge et al. from experiment perspective[19] showed that solvated cation in the electrolyte could induce a large local negative electric field of up to −1 V/Å. Both microkinetic model and experiments showed that such a strong negative field could enhance CO_2RR-to-CO.

The mechanism of CO_2 initial activation is still unclear in the current field. Two possible mechanisms include concerted proton-electron transfer (CPET, an electrochemical reaction involving proton exchange) and proton transfer with molecule bound CO_2^{-}.[20] In this work we followed CPET pathway[8] because CPET is usually applied for metallic catalysts (i.e., Cu-based catalysts[21]). Aminothiolate SAM-modulated Cu catalysts provide an organic active site to the first proton-electron transfer to CO_2 – one possible RDS affecting CO_2RR activity (Figure 1b) [Eq. (1)].[6,8]

$$CO_2(gas) + H^* \rightarrow COOH^* \quad (1)$$

Here, van der Waals correction was taken into account to involve the weak interaction between various coverages of

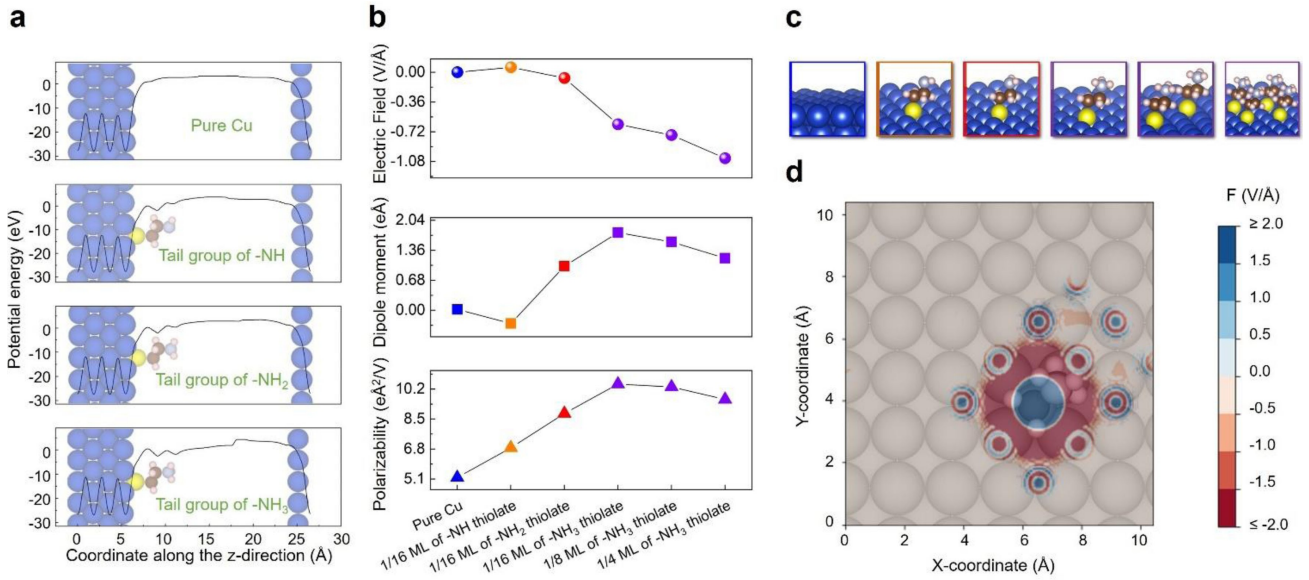

Figure 3. a Schematic illustration of the electronic properties of aminothiolate SAM-modulated Cu catalysts; **b** The induced average electric field, dipole moment and polarizability of catalysts, i.e., pure Cu (blue), –NH thiolate/Cu (orange), $–NH_2$ thiolate/Cu (red), and $–NH_3$ thiolate/Cu (purple) at various surface coverages; **c** The side views of the optimized catalyst geometries in **b**; **d** The local electric field near Cu(100) (x-y contour plot of S atom) induced by aminothiolate at 1/16 ML.

aminothiolates. Our results show that the presence of aminothiolates increases CO_2 physisorption energy compared to the bare Cu (Figures S9–S11 and Table S2). In addition, CO_2 activation on an organic N site has lower reaction energy compared to that on an inorganic Cu site by up to 1.9 eV (Figure 4a). This is because there is more electron transfer between COOH* and organic N site of aminothiolate than COOH* and inorganic Cu site (Figure 4b). As the coverage of aminothiolate increases to 1/2 ML, COOH* formation energy decreases 1.6 eV over Cu(100), 0.36 eV over Cu(111) and 0.38 eV over Cu(211), indicating that a higher coverage of aminothiolate SAMs over Cu catalyst favors CO_2 initial activation (Figures S12–S14). This is because the hydrogen bond length between aminothiolates and COOH* decreases at a higher coverage of aminothiolates, resulting in a stronger hydrogen bond effect (Figure S15). Compared to Cu(111) and (211), COOH* formation energy over (100) drops significantly, because Cu(100) is less compact than Cu(111) and (211) and thus, aminothiolates over Cu(100) at 1/2 ML have the smallest lateral interaction. Similar findings were observed from the existing experimental and theoretical literature. Experimentally, Zhang et al.[11a] investigated CO_2 reduction to CO over phosphonic acid monolayers (RPO_3H_2) modulated Pt or Pd catalysts. They found that replacing the functional group –R to $–NH_2$ within the RPO_3H_2 monolayers could lead to a stronger CO_2 adsorption and a higher hydrogenation reactivity. Meng et al.[11b] studied CO_2 electroreduction to CO (CO_2RR-to-CO) over amino-modified polymeric carbon nitride (PCN). They showed that the reaction rate of CO_2RR-to-CO over amino-modified PCN increased by 17-fold as compared to that over unmodified PCN. Bacsik et al.[11c] studied CO_2 capture using *n*-propylamines modified silica. They found that CO_2 reacted with amine group and formed ammonium carbamate ion pairs. At a high density of amine groups, the ammonium carbamates could further be stabilized to form carbamic acids via the H-bond with the adjacent amine group. Theoretically, Xiao et al.[11d] performed DFT calculations of CO_2 adsorption thermodynamics over N-substituted/grafted graphane. They found that via forming the H-bond and the strong C–N bond, CO_2 adsorption could be greatly enhanced with the presence of $–NH_2$ site on graphane.

Interestingly, the SAM-modulated Cu catalysts provide dual organic-inorganic active sites (–NH and Cu) for the potential RDS of C–C coupling [Eq. (2)][6,12] during CO_2RR-to-C_2 (Figure 1b).

$$CO^* + COH^* \rightarrow OCCOH^* + * \quad (2)$$

The adsorption sites for CO*, COH* and OCCOH* are determined by the energetic comparison. DFT results show that at 1/16 ML of aminothiolate, CO* adsorbed on inorganic Cu site is ~2 eV more stable than that over organic –NH site; the adsorption energy of COH* and OCCOH* over –NH site is ~2 eV more stable than that over a Cu site (Figures S16–S19). The reaction energies of C–C coupling (Equation (S24) in the SI) in the presence of aminothiolates at 1/16 ML are greater than that on the pristine Cu, suggesting C–C coupling is thermodynamically less favorable (Figure 5a and Figures S20–S22). As the surface coverage of aminothiolates increases to 1/4 ML, the reaction energy of C–C coupling decreases monotonically because: **(1)** The final state OCCOH* is stabilized via the H-bond from the adjacent amine group. Specially, the H-bond effect at 1/4 ML is stronger than that at 1/8 ML because the shorter H-bond length forms at 1/4 ML of SAMs (Table S3). It is also noted that there isn't H-bond effect with 1/8 ML of SAMs over Cu(100). This is because Cu(100) is a less densely packed surface and thus the distance between OCCOH* and the adjacent amine group is too far to form the H-bond. This explains why the reaction energy of C–C coupling over Cu(100) remains nearly unchanged when the coverage increases from 1/16 ML to 1/8 ML. **(2)** The induced confinement effect could enforce CO* to its less stable adsorption site over Cu and decrease its adsorption energy; Specially, CO* is enforced to move from top site to hollow site over Cu(100); from the hollow site to the bridge site over Cu(111); and from the step site to the terrace site over Cu(211) at 1/4 ML of aminothiolates (Figure S23). This is consistent with the previous study[9c] that the confinement effect induced by C_{18} thiols decreased the adsorption energy of the reactant and thus changed the selectivity. **(3)** The adsorption energy of the other key intermediate CO* over the organic –NH site (i.e., in the format of COH*) is stabilized via the strong C–N bond. Thus, the adsorption energy difference between CO* and COH* enlarges (Figures S24–S25), which consequently, decreases the reaction energy of the C–C coupling and promotes CO_2RR-to-C_2. This finding is consistent

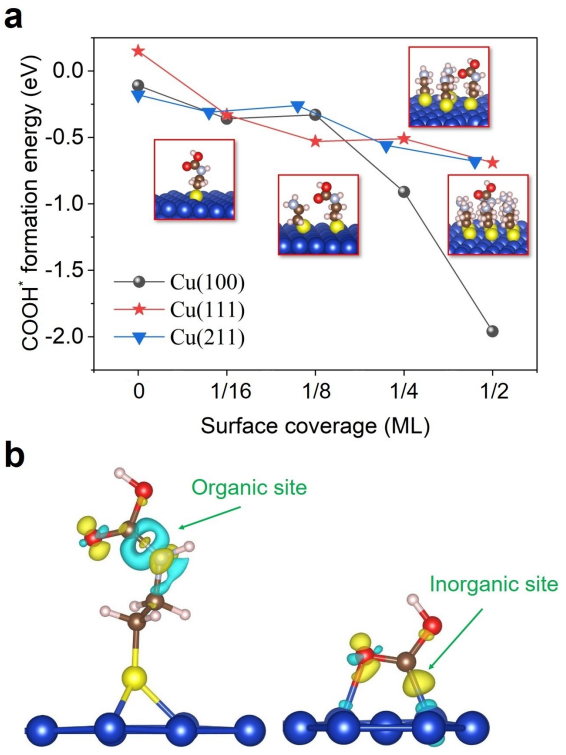

Figure 4. a CO_2 initial activation over aminothiolate SAM-modulated Cu catalysts. The optimized geometries of Cu(111) case are inserted; **b** Differential charge density of COOH* on inorganic Cu site and organic N site. The iso-surface level of the differential charge density is 0.013 e/bohr. The yellow and blue area denote gain and loss of electrons, respectively.

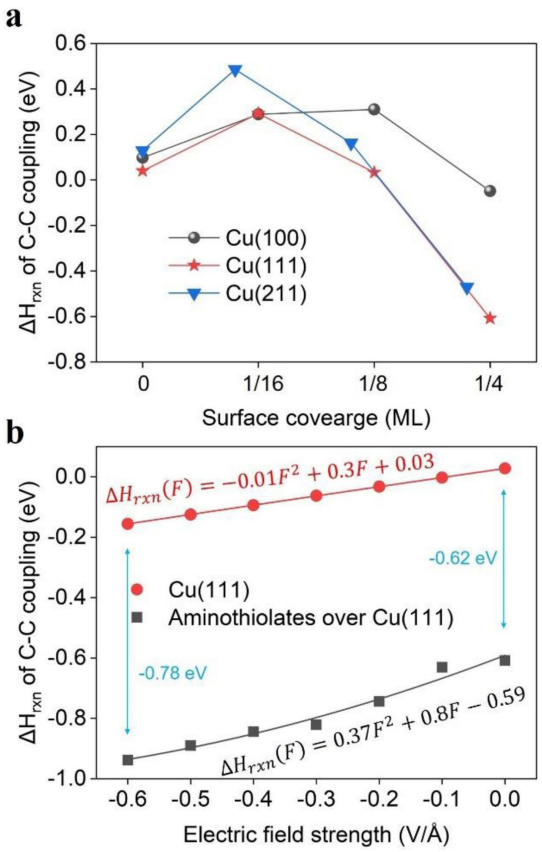

Figure 5. a The reaction energy of C–C coupling ($CO^* + COH^* \rightarrow OCCOH^*$) over Cu(100), Cu(111), and Cu(211) as function of surface coverages of aminothiolate SAMs. **b** Electric field effects on the reaction energy of C–C coupling over Cu(111) with and without 1/4 ML aminothiolate SAMs.

with literature from Zhou et al.[22] and Xiao et al.[23] that the larger difference in the adsorption energies of two CO* during C–C coupling step led to a lower reaction energy and activation barrier of C–C coupling and a better selectivity of CO_2RR-to-C_2. Collectively, hydrogen bond and confinement effects induced by high coverages of SAMs dramatically decreases the reaction energies of C–C coupling by up to ~0.6 eV as compared to the pure Cu (Figure 5a). The aminothiolates with a surface coverage of 1/2 ML poison the surface since all Cu active sites are fully occupied by aminothiolates, leaving no available sites for CO*. Therefore, the selectivity of CO_2RR-to-C_2 over aminothiolate SAM-modulated Cu behaves as "volcano-like" plot: (1) aminothiolates provide dual organic (i.e., –NH) – inorganic (i.e., Cu) surface active sites; (2) the hydrogen bond helps stabilize OCCOH*; (3) aminothiolates induce confinement effects at 1/4 ML, affecting the site selection of a key intermediate (i.e., CO*) and enlarges the adsorption energies of CO and COH.

A homogeneous negative electric field, up to the order of 1 V/Å,[18,24] exists at the electrode/electrolyte interface during electrocatalysis. Thus, we applied an external negative electric field to C–C coupling over Cu with and without aminothiolate SAMs (Figure 5b). The reaction energies ($\Delta H_{rxn}(F)$) of C–C coupling as a function of electric fields (F) can be analyzed using a Taylor expansion [Eq. (3)]

$$\Delta H_{rxn}(F) = \Delta H^0_{rxn} - \Delta\vec{d}\cdot\vec{F} - \frac{1}{2}\Delta\alpha\cdot\vec{F}^2 \quad (3)$$

where $\Delta\vec{d}$, $\Delta\alpha$ are the changes of the dipole moment and polarizability between the initial and final states and ΔH^0_{rxn} is the reaction energy without electric fields. Since the aminothiolate SAMs induce significant changes in the $\vec{d}$ and α of Cu, $\Delta H_{rxn}(F)$ is remarkably different with and without aminothiolates. Notably, when the electrode/electrolyte interfacial electric field is absent, SAMs can decrease the reaction energy of C–C coupling by 0.62 eV; at an interfacial electric field of -0.6 V/Å, SAMs can further descrease the reaction energy of C–C coupling by 0.78 eV, meaning the changed dipole moment and polarizability are able to further promote C–C coupling under electrochemical environment (Figure 5b).

We lastly examined HER (Figure 1b) by calculating the free energy of H* and comparing it to the HER volcano plot in the literature.[25] All Cu facets inhibit HER when the aminothiolate coverage reaches a higher coverage (i.e., 1/4 ML) (Figure S26). Our result agrees well with Banerjee et al.'s study,[26] in which higher concentration of cetyltrimethylammonium bromide (CTAB) has shown the ability to suppress HER because of the increased double layer capacitance. More details regarding HER, computational methods of electric fields and their effects on energy analysis are given in SI.

Collectively, our work guides novel catalyst designs, i.e., SAM-modulated catalysts, which provide organic-inorganic dual active sites, hydrogen bond effect, confinement effects, highly localized electric fields and changes in the catalyst surface's dipole moments and polarizability, thus potentially enabling more efficient energy utilization and CO_2 conversion efficiency to C_2 than that obtained with conventional catalyst designs. This theoretical research provides an innovative picture of electrocatalysis at hybrid organic-inorganic interfaces, and specifically their roles in increasing the catalytic activity and selectivity. The outcomes of this research will be transformative to other electrocatalytic reactions that suffer from weak reactant adsorption and adsorption-sensitive selectivity (e.g., CH_4 conversion to methanol, nitrogen reduction reaction) and SAM-modulated thermal catalysis.

Acknowledgements

This work was partially supported by institutional faculty start-up funds from University of Massachusetts Lowell. Our thanks also go to the National Science Foundation for partial support (award #2103478). The authors also acknowledge the computational resources provided by Massachusetts Green High Performance Computing Center (MGHPCC) and Texas Advanced Computing Center (TACC). We thank Dr. Alyssa J.R. Hensley and Dr. Jun Li for their helpful comments.

Conflict of Interest

The authors declare no conflict of interest.

Keywords: Density function calculations · Electrochemistry · Self-assembly

[1] M. Jouny, W. Luc, F. Jiao, *Ind. Eng. Chem. Res.* **2018**, *57*, 2165–2177.
[2] A. Vasileff, Y. Zheng, S. Z. Qiao, *Adv. Energy Mater.* **2017**, *7*, 1700759.
[3] Y. Y. Birdja, E. Pérez-Gallent, M. C. Figueiredo, A. J. Göttle, F. Calle-Vallejo, M. T. M. Koper, *Nat. Energy* **2019**, *4*, 732–745.
[4] S. Nitopi, E. Bertheussen, S. B. Scott, X. Liu, A. K. Engstfeld, S. Horch, B. Seger, I. E. L. Stephens, K. Chan, C. Hahn, J. K. Norskov, T. F. Jaramillo, I. Chorkendorff, *Chem. Rev.* **2019**, *119*, 7610–7672.
[5] M. B. Ross, P. De Luna, Y. Li, C.-T. Dinh, D. Kim, P. Yang, E. H. Sargent, *Nat. Catal.* **2019**, *2*, 648–658.
[6] R. Kortlever, J. Shen, K. J. Schouten, F. Calle-Vallejo, M. T. Koper, *J. Phys. Chem. Lett.* **2015**, *6*, 4073–4082.
[7] S. Jin, Z. Hao, K. Zhang, Z. Yan, J. Chen, *Angew. Chem. Int. Ed.* **2021**, *60*, 20627–20648.
[8] J. S. Yoo, R. Christensen, T. Vegge, J. K. Norskov, F. Studt, *ChemSusChem* **2016**, *9*, 358–363.
[9] a) S. H. Pang, C. A. Schoenbaum, D. K. Schwartz, J. W. Medlin, *Nat. Commun.* **2013**, *4*, 2448; b) C. A. Schoenbaum, D. K. Schwartz, J. W. Medlin, *J. Catal.* **2013**, *303*, 92–99; c) L. O. Mark, C. Zhu, J. W. Medlin, H. Heinz, *ACS Catal.* **2020**, *10*, 5462–5474; d) C.-H. Lien, J. W. Medlin, *J. Phys. Chem. C* **2014**, *118*, 23783–23789.
[10] L. D. Ellis, R. M. Trottier, C. B. Musgrave, D. K. Schwartz, J. W. Medlin, *ACS Catal.* **2017**, *7*, 8351–8357.
[11] a) J. Zhang, S. Deo, M. J. Janik, J. W. Medlin, *J. Am. Chem. Soc.* **2020**, *142*, 5184–5193; b) N. Meng, W. Zhou, Y. Yu, Y. Liu, B. Zhang, *ACS Catal.* **2019**, *9*, 10983–10989; c) Z. Bacsik, N. Ahlsten, A. Ziadi, G. Zhao, A. E. Garcia-Bennett, B. Martin-Matute, N. Hedin, *Langmuir* **2011**, *27*, 11118–11128; d) J. Xiao, S. Sitamraju, M. J. Janik, *Langmuir* **2014**, *30*, 1837–1844.
[12] H. Xiao, T. Cheng, W. A. Goddard, 3rd, *J. Am. Chem. Soc.* **2017**, *139*, 130–136.
[13] a) M. Luo, J. Frechette, *J. Phys. Chem. C* **2010**, *114*, 20167–20172; b) J. Lahann, S. Mitragotri, T.-N. Tran, H. Kaido, J. Sundaram, I. S. Choi, S. Hoffer, G. A. Somorjai, R. Langer, *Science* **2003**, *299*, 371–374; c) J.-S. Park, A. N. Vo, D. Barriet, Y.-S. Shon, T. R. Lee, *Langmuir* **2005**, *21*, 2902–2911; d) P. Maksymovych, D. C. Sorescu, J. T. Yates, Jr., *Phys. Rev. Lett.* **2006**, *97*, 146103; e) A. Kühnle, S. Vollmer, T. R. Linderoth, G. Witte, F. Besenbacher, *Langmuir* **2002**, *18*, 5558–5565; f) S. M. Driver, D. P. Woodruff, *Surf. Sci.* **2001**, *488*, 207–218.
[14] C. R. Bernard Rodriguez, J. A. Santana, *J. Chem. Phys.* **2018**, *149*, 204701.
[15] G. Schkolnik, J. Salewski, D. Millo, I. Zebger, S. Franzen, P. Hildebrandt, *Int. J. Mol. Sci.* **2012**, *13*, 7466–7482.
[16] F. Che, J. T. Gray, S. Ha, J.-S. McEwen, *ACS Catal.* **2017**, *7*, 6957–6968.
[17] S. Sarkar, A. Maitra, S. Banerjee, V. S. Thoi, J. M. Dawlaty, *J. Phys. Chem. B* **2020**, *124*, 1311–1321.
[18] L. D. Chen, M. Urushihara, K. Chan, J. K. Nørskov, *ACS Catal.* **2016**, *6*, 7133–7139.
[19] C. M. Gunathunge, V. J. Ovalle, Y. Li, M. J. Janik, M. M. Waegele, *ACS Catal.* **2018**, *8*, 7507–7516.
[20] J. Shen, M. J. Kolb, A. J. Göttle, M. T. M. Koper, *J. Phys. Chem. C* **2016**, *120*, 15714–15721.
[21] A. J. Gottle, M. T. M. Koper, *Chem. Sci.* **2017**, *8*, 458–465.
[22] Y. Zhou, F. Che, M. Liu, C. Zou, Z. Liang, P. De Luna, H. Yuan, J. Li, Z. Wang, H. Xie, H. Li, P. Chen, E. Bladt, R. Quintero-Bermudez, T. K. Sham, S. Bals, J. Hofkens, D. Sinton, G. Chen, E. H. Sargent, *Nat. Commun.* **2018**, *10*, 974–980.
[23] H. Xiao, W. A. Goddard, 3rd, T. Cheng, Y. Liu, *Proc. Natl. Acad. Sci. USA* **2017**, *114*, 6685–6688.
[24] M. J. Hulsey, C. W. Lim, N. Yan, *Chem. Sci.* **2020**, *11*, 1456–1468.
[25] J. K. Nørskov, T. Bligaard, A. Logadottir, J. R. Kitchin, J. G. Chen, S. Pandelov, U. Stimming, *J. Electrochem. Soc.* **2005**, *152 (3)*, J23.
[26] S. Banerjee, X. Han, V. S. Thoi, *ACS Catal.* **2019**, *9*, 5631–5637.

Manuscript received: August 18, 2021
Revised manuscript received: October 29, 2021
Accepted manuscript online: November 10, 2021
Version of record online: December 2, 2021